Journal of Engineering Science and Technology
23rd EURECA 2025 Special Issue February (2026) 51 - 62

DESIGN AND DEVELOPMENT OF A PLA RECYCLING MACHINE FOR 3D PRINTER FILAMENT PRODUCTION

J. K. LOH[1], P. X. KU[1,*], H. L. CHOO[1], N. Z. ABU BAKAR[1], P. P. AUNG[2]

[1]School of Engineering, Faculty of Innovation and Technology, Taylor's University, Selangor, Malaysia
[2]Faculty of Engineering and Technology, Sunway University, Malaysia
*Corresponding Author: peixuan.ku@taylors.edu.my

Abstract

The rapid growth of fused deposition modelling has increased demand for polymer filament and contributed to rising plastic waste. Polylactic acid (PLA) is the most widely used filament due to its ease of printing and bio-based origin, yet it does not readily degrade under normal landfill conditions, leading to environmental concerns. This study presents a desktop-scale, open-source recycling machine designed to convert waste PLA into new filament for additive manufacturing. The system integrates a modular aluminium extrusion frame, 3D printed subassemblies, and Arduino-based dual-zone proportional-integral-derivative temperature control. Recycled PLA filament was evaluated through filament dimensional, energy, and cost analyses. Results showed that recycled PLA achieved an average diameter of 1.77 ± 0.07 mm, with fluctuations ranging from 1.3 mm to 2.4 mm. Although drying accounted for ~95% of energy usage, production remained cost-effective at RM 5.31/kg, with breakeven achieved after ~19 kg of filament. The findings confirm the technical and economic viability of distributed PLA recycling and highlight its potential to sustainable practices in additive manufacturing.

Keywords: Additive manufacturing, rPLA, Open-source hardware, PLA recycling, Sustainable filament.

1. Introduction

The rapid adoption of additive manufacturing, particularly fused deposition modelling (FDM), has driven a surge in polymer filament consumption and plastic waste generation. Polylactic acid (PLA) is the most widely used material due to its ease of printing, bio-based origin, and low toxicity [1]. In Malaysia, PLA represents over 85% of filament consumption among hobbyists, educators, and small-scale industrial users [2]. Despite its reputation as biodegradable, PLA requires industrial composting facilities that are not widely available, and it persists under typical landfill conditions, contributing to waste accumulation and potential microplastic pollution [3].

Mechanical recycling provides a practical strategy to extend PLA's material life cycle while reducing environmental impacts. Failed prints and offcuts can be reprocessed into new filament, supporting circular use of resources. Several open-source and commercial systems, such as the Lyman extruder, RecycleBot, and Filabot, have demonstrated the viability of distributed filament recycling [4, 5]. However, these solutions often suffer from high cost, limited modularity, and inconsistent product quality due to unstable thermal management and the absence of closed-loop diameter control [6].

In addition to reducing waste, desktop-scale recycling offers significant economic and social benefits. By producing filament in-house, users can lower material costs, reduce dependence on supply chains, and gain greater control over their production processes [7]. The integration of recycling into makerspaces, schools, and small enterprises also promotes awareness of sustainable practices and fosters innovation in material reuse [8]. Such benefits highlight the broader potential of distributed recycling to transform additive manufacturing into a more circular and resilient system.

Nevertheless, current recycling technologies face several critical limitations. High energy consumption during pre-processing, significant variation in filament diameter, and a lack of affordable, user-friendly systems restrict their practical adoption [5, 7, 8]. These challenges highlight the need for a compact, modular, and low-cost solution capable of producing consistent filament quality with minimal operator intervention. Therefore, this objective of this paper is to design and develop a desktop-scale, open-source PLA recycling machine that addresses these gaps and supports sustainable additive manufacturing. The system is designed to integrate an aluminium extrusion frame with 3D printed subassemblies for extrusion, cooling, and spooling. A dual-zone temperature control system using Arduino-based proportional-integral-derivative (PID) loops ensures stable extrusion conditions, while filament pulling are optimised to minimise diameter variation. The machine also incorporates safety logic, simplified user maintenance, and a compact footprint for desktop use.

2. Method

2.1. Feedstock preparation

Waste PLA was collected from failed prints, support structures, and offcuts generated in the 3D printing laboratory at Taylor's University. The material was manually sorted to remove contaminants and then size-reduced using a high-torque blender to produce uniform flakes suitable for extrusion. As PLA is hygroscopic, Feedstock was oven-dried at 60 °C for 12 h in a Memmert UN75 convection oven to minimise hydrolytic degradation during processing, with weight loss used to confirm drying efficiency. Table 1 summarises the drying parameters for different sample batches. Drying at 65 °C for 4 h was selected as a faster approach, while extended drying at 60 °C for 12-18 h was employed as a gentler method to minimise the risk of thermal degradation. A weight reduction of 0.01-0.5% was taken as the criterion for adequate drying of PLA flakes [9, 10]. The drying process ensured that the moisture content was reduced to below 250 ppm, thereby preventing degradation during subsequent extrusion (Fig. 1).

Additionally, PLA fragments smaller than 1 mm were excluded from extrusion to avoid nozzle clogging; these fine particles were instead upcycled into flat PLA sheets by oven-heating at 170 °C for 20 min, producing durable components for secondary applications such as coasters or structural spacers.

Table 1. Drying parameters for PLA samples.

Sample	Duration (hours)	Temperature (°C)	Mass (Before) (g)	Mass (After) (g)	Percentage loss (%)
A	4	65	184.2	183.6	0.33
B	12	60	477.3	476.4	0.19
C	18	60	2344.81	2338.93	0.25

(a) Oven-dried PLA flakes.

(b) Post-drying mass measurement.

Fig. 1. PLA drying procedure.

2.2. System architecture and components

2.2.1. Extruder and mechanical integration

The extrusion system was designed to be modular, compact, and cost-effective. The primary frame was constructed from 20 × 100 mm aluminium extrusions, providing structural rigidity while allowing straightforward assembly, disassembly, and integration of interchangeable modules. The subassemblies such as extruder barrel, filament puller, water bath were modelled in SolidWorks (Version 2023) and subsequently fabricated using a Raise3D Pro Plus FDM printer.

The feed mechanism used a modified wood auger (460 mm length, 20 mm outer diameter) housed within a 19 mm steel barrel (Fig. 2). Thrust bearings and custom 3D-printed mounts were incorporated to maintain rotational alignment and manage axial loads during operation. Power was supplied by a worm-gear wiper motor, coupled to the auger through a shortened 12 mm socket, which functioned both as a direct-drive interface and as a quick-release coupling in the event of filament blockage. The extruder terminated in a GI pipe endcap drilled to 1.5-2.0 mm, which served as the die. A stainless-steel mesh filter was positioned upstream of the nozzle to capture residual solid impurities and promote partial melt homogenisation. Incorporation of melt filtration significantly improved the surface finish of the extrudate and reduced particulate inclusions in the final filament.

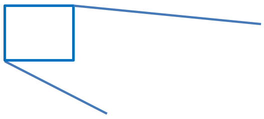

Fig. 2. 3D model of the assembled recycling system with cross-sectional view of auger in extrusion section.

2.2.2. Temperature control and heating system

The extruder barrel was equipped with two 200 W band heaters, distributed across the feed and die zones. Temperature regulation was implemented using MAX6675 thermocouple modules interfaced with an Arduino Mega 2560 microcontroller. Each zone was independently controlled via PID control loops, with SSR-25DA solid-state relays modulating heater output through pulse-width modulation signals. PID parameters were tuned using step-response analysis and final gains for Heater 1 (feed zone) and Heater 2 (die zone) are shown Table 2.

Table 2. Final PID gains for each heater zone.

Heater	Proportional gain, K_p	Integral gain, K_i	Derivative gain, K_d
1	11.318	0.179	178.634
2	12.062	0.185	196.422

A thermal runaway protection protocol was implemented through a failsafe logic loop that automatically disabled the heaters if the thermocouple signal was absent, unstable, or exceeded 250 °C. External validation using a handheld multimeter thermoprobe confirmed the accuracy of Arduino-controlled measurements within ±1.5 °C. The complete circuit schematic with all components is illustrated in Fig. 3.

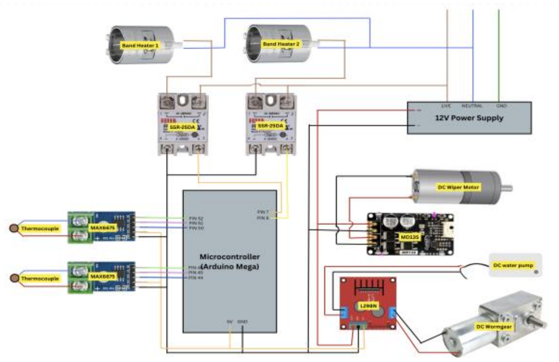

Fig. 3. Circuit schematic for the rPLA recycling machine.

2.2.3. Filament cooling and pulling mechanism

The extruded filament was passed through a water bath located 30 mm downstream of the die to promote rapid cooling and dimensional stabilisation (Fig. 4(a)). Filament transport was achieved using a dual-roller pulling mechanism driven by a 40 rpm DC worm-gear motor (Fig. 4(b)). The rollers were lined with elastic tape and rubber bands to form a V-groove profile, which improved grip and facilitated self-alignment of the filament. A belt drive system was selected over direct coupling to minimise torque ripple and absorb transient loads arising from filament irregularities. The pulling speed was manually controlled via a potentiometer, allowing the filament diameter to be maintained within 1.70-1.80 mm.

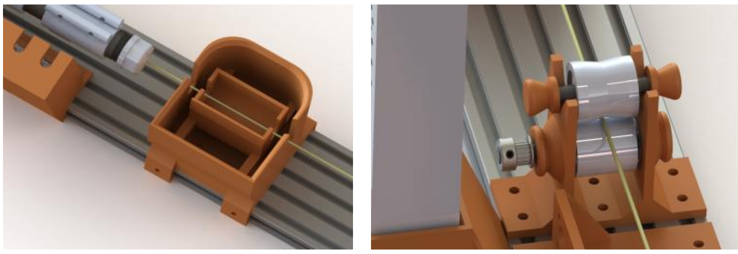

(a) Water bath. **(b) Pulling mechanism.**

Fig. 4. Filament cooling and pulling systems.

2.3. Filament diameter consistency

Upon assembly of the recycling system, recycled polylactic acid (rPLA) filament was extruded. Filament samples from three independent extrusion runs (Set 1, Set 2, and Set 3) were measured at 5 cm intervals along 100 cm strands using a digital caliper with a resolution of ±0.01 mm. At each interval, averaged readings across two perpendicular diameters were recorded as D_1 and D_2 to account for cross-sectional ovality. Three commercially available virgin polylactic acid (vPLA) filaments (grey, yellow, white) were measured as control specimens under identical settings.

2.4. Energy and cost analysis

Energy consumption was evaluated for both the feedstock drying and extrusion phases. The drying oven was assumed to operate at a 40% duty cycle once the setpoint temperature was reached, corresponding to an average power draw of 960 W over a 12 h cycle. Extrusion energy usage was profiled by logging duty cycles and component loads, with the barrel heaters drawing 40-100% of their 200 W rating and the motors operating between 2-20 W. Table 3 presents the component duty cycles during start-up and continuous operation, alongside their rated power

The total energy required to produce 1 kg of rPLA was calculated by summing the drying and extrusion contributions, as expressed in Eq. (1):

$$E_{total} = E_{drying} + E_{extrusion} \quad (1)$$

The production cost per kilogram was derived using Malaysia's residential electricity tariff of RM 0.454/kWh. For economic benchmarking, the calculated cost was compared against the current market price of vPLA (RM 45/kg) to calculate the breakeven points and potential savings.

Table 3. Component duty cycles and corresponding rated power for extrusion operation.

Stage	Startup Usage (%)	Operational Usage (%)	Rated Power (W)
Barrel heater 1	100	40	200
Barrel heater 2	20	Off	200
Extrusion motor	Off	100	19.68
Puller motor	Off	50	2
Water pump	Off	100	1
Logic board	Active	Active	0.5

3. Results and Discussion

3.1. Extruder performance

The prototype was assembled and operated according to the design specifications (Fig. 5). The key subsystems: the extruder barrel, dual-zone heating, puller mechanism, and water bath, functioned cohesively to produce continuous rPLA filament. The extrusion trials revealed several design sensitivities.

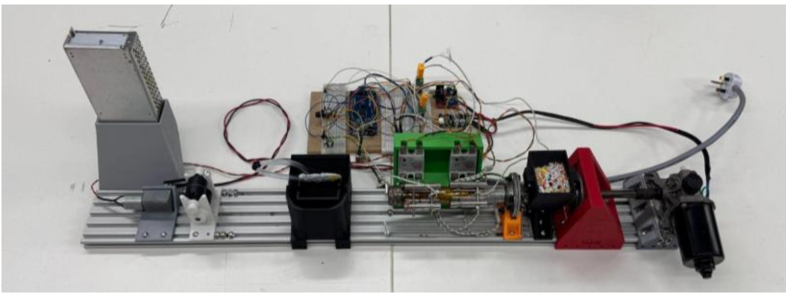

Fig. 5. Assembled prototype of the rPLA recycling machine.

The nozzle diameter was found to strongly influence melt flow behaviour and extrusion stability. The 1.5 mm die frequently caused pressure buildup and clogging due to restricted melt throughput, whereas the 2.0 mm die provided smoother flow and more uniform filament formation. This observation is consistent with reports that nozzle geometry governs pressure drop and shear rate distribution, particularly in viscoelastic polymer melts such as PLA [11]. Moreover, integrating a melt filter upstream of the die enhanced filament surface quality by removing impurities and promoting partial homogenisation of the melt. This highlights the critical role of pre-die filtration in reducing surface roughness and ensuring consistent extrusion quality.

Thermal stability also played a decisive factor influencing the extruder performance. When untreated PLA flakes were processed, extrusion consistently resulted in severe bubbling, embrittlement, and poor filament cohesion (Fig. 6). These defects are attributed to hydrolytic chain scission, where absorbed moisture accelerates polymer degradation during heating, reducing molecular weight and viscosity [12].

In contrast, pre-dried PLA produced continuous, bubble-free strands with a smoother surface finish, emphasising the necessity of rigorous drying protocols. Because PLA is highly sensitive to moisture and exhibits low resistance to hydrolysis, the control of moisture content in rPLA flakes is essential [13]. Residual moisture can promote chain scission, resulting in poor surface finish, brittleness, and inconsistent filament diameter during extrusion [14, 15]. Quader et al. [16] found that moisture exposure significantly degraded PLA 4043D filaments, causing a 20% reduction in tensile strength and a 50% increase in melt flow index.

Conversely, Algarni [17] reported that reducing the moisture content from 10% to 1% decreased the ultimate tensile strength of PLA by 24.4%. He suggested that this is mainly due to the loss of ductility as the moisture content decreased. These contrasting findings indicate that while excessive moisture clearly promotes hydrolytic degradation and weakens PLA during extrusion, excessive drying can also alter material behaviour by reducing ductility.

Besides, the cooling and pulling subsystems may also affect dimensional stability. The 30 mm downstream water bath facilitated rapid solidification, reducing filament swelling and ovality. However, variations in pulling speed led to diameter fluctuations, with deviations directly correlated to roller slippage and transient motor loading. The use of elastic tape and rubber bands to create a V-groove profile improved filament centering, yet diameter consistency remained partly dependent on user adjustment. This is consistent with broader limitations observed in distributed recycling systems lacking closed-loop diameter control [18].

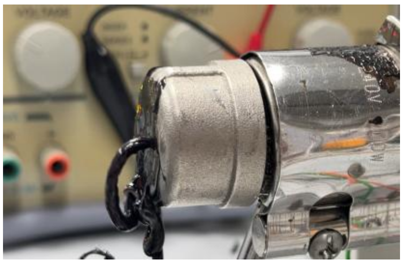

Fig. 6. Extruded rPLA filament.

3.2. Filament quality

In this study, the filament diameter measurements of rPLA were obtained from three independent extrusion runs (Set 1, Set 2, and Set 3). Each strand was measured along 100 cm segments at two perpendicular orientations (D_1 and D_2) to account for cross-sectional ovality.

The findings show noticeable variation both within and between extrusion runs. Set 1 exhibited relatively stable diameters, with values clustering around 1.6–2.0 mm, though local fluctuations were observed (Fig. 7). Set 2 showed the largest deviations, with diameters ranging between 0.8 mm and 2.0 mm, indicating intermittent thinning and thickening along the filament length. In contrast, Set 3 produced thicker strands overall, with values between 1.5 mm and 2.6 mm, before gradually tapering towards ~1.0 mm at the filament end.

Moreover, the rPLA filament diameter tends to vary along the 100 cm segments. Commercial vPLA exhibited an average diameter of 1.75 ± 0.03 mm, which is consistent with typical manufacturer tolerances (Fig. 8). In comparison, rPLA produced by the extruder system exhibited greater fluctuations, ranging from 1.3 mm to 2.4 mm along the 1 m segment. The diameter initially exceeded 2.0 mm within the first 20 cm, then gradually decreased, with notable instability beyond 60 cm. Although the variation slightly exceeded the ±0.05 mm tolerance band generally recommended for high-precision FDM printing, the rPLA filament remained within an acceptable range for standard applications, indicating its practical usability in non-critical prototyping and educational contexts.

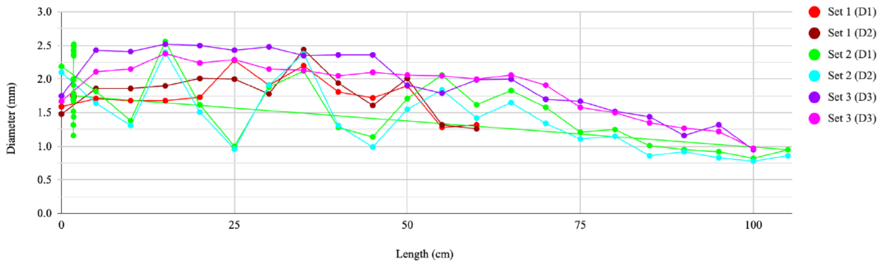

Fig. 7. Filament diameter over length.

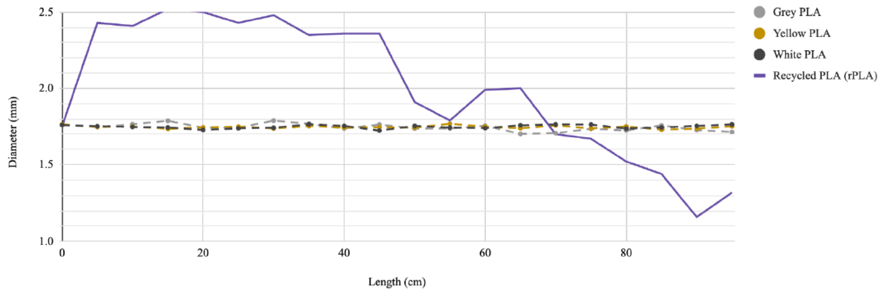

Fig. 8. Comparison of vPLA vs rPLA diameter consistency.

These inconsistencies suggest that extrusion stability was influenced by both process parameters and mechanical dynamics. Variations in pulling speed and roller grip likely contributed to local diameter spikes, while insufficient cooling time before the water bath may have caused filament swelling or necking. The observed tapering trend, especially in Set 3, may be linked to thermal drift in the barrel or gradual changes in auger throughput over time.

Despite these fluctuations, the average filament diameter across sets remained close to the nominal 1.75 mm specification. However, the spread exceeded the ±0.05 mm tolerance generally expected for commercial-grade filament, highlighting the limitations of manual pulling and the absence of closed-loop control. These findings align with prior reports on distributed recycling systems such as the RecycleBot and Filabot, where dimensional stability is largely dependent on haul-off and cooling control rather than extrusion alone [5, 19].

To systematically address these challenges, a series of process refinements were implemented. Table 4 summarises the main interventions and their impact on filament quality.

Table 4. Process adjustments and their effect on filament extrusion quality.

Parameter	Initial Condition (Before)	Improved Outcome (After)
Addition of melt filter	Filament prone to break due particulate contamination	Stronger, continuous filament that withstands spooling
Drying of PLA pellets	Bubbling, steam pockets and irregular flow	Smooth, bubble-free extrusion with improved cohesion
Increased extrusion die diameter	1.5 mm die clogs frequently; high torque causes motor stalling	2.0 mm die provides smoother flow; motor operates without overload
Reduced barrel temperature	Excessive extrusion speed led to poor cooling and deformation	Slower, more controlled extrusion enabling proper solidification
Addition of cooling fan	Filament remained semi-molten, difficult to transfer to water bath	Faster surface solidification and easier filament handling

3.3. Energy consumption

Energy usage was profiled across the startup, extrusion, and drying phases. Startup heating consumed 26.4 Wh to raise the barrel to the operating temperature (around 190 °C). During continuous extrusion, the average power draw stabilised at 102 W, resulting in 0.212 kWh to produce 1 kg of filament at a throughput of 550 g/h. The drying stage was the dominant energy consumer, requiring 12.1 kWh for a 1 kg batch of PLA flakes when operated at 60 °C for 12 hours. Table 5 summarises the energy distribution.

Table 5. Energy consumption to produce 1 kg of rPLA.

	Startup (Wh)	Operational power (W)	Duration (hours)	Total energy used (kWh)
Prototype	26.44	102.18	1.818	0.2122
Feedstock drying	600	960	12	12.120

Energy analysis revealed that filament drying was by far the dominant contributor, accounting for approximately 93.4% of the total energy required to produce 1 kg of rPLA. In contrast, prototype operation during extrusion represented only 1.5%, while startup heating of the extruder barrel contributed 0.2%. Oven startup added another 4.9%. Together, these results show that nearly all of the energy demand originates from the drying process, with extrusion and startup phases making only marginal contributions.

Thus, the total energy footprint for producing 1 kg of rPLA was 12.3 kWh, of which 95% was attributed to drying. Similar findings have been reported in other small-scale systems, where feedstock preparation outweighs extrusion in energy intensity [6]. Further optimisation of energy usage can be achieved through the integration of desiccant-based drying systems or alternative low-energy drying methods.

3.4. Economic feasibility

The complete build cost of the prototype was RM 746.34, substantially lower than commercial filament extruders such as the Filabot, which retail between USD 900 and 3,500. Based on measured energy and material inputs, the production cost of rPLA was estimated at RM 5.31/kg, compared to approximately RM 45/kg for vPLA sourced from commercial suppliers. At this cost differential, the system reaches breakeven after the production of ~19 kg of filament, equivalent to less than one month of moderate use in an educational makerspace.

Although the drying stage represented the dominant share of energy demand, the overall economics remain favourable. For example, producing 100 kg of filament would yield cumulative savings of over RM 3,900 relative to purchasing vPLA, even without further optimisation. Such savings scale significantly in high-throughput environments such as universities, research labs, and community workshops. These findings confirm that distributed recycling system can provide a cost-effective and sustainable alternative to commercial filament purchases. Accumulated savings vs rPLA produced is shown in Fig. 9.

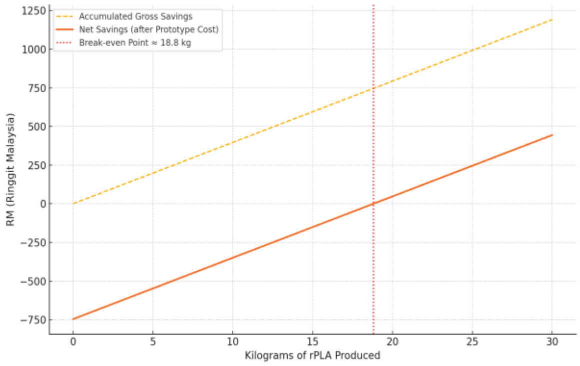

Fig. 9. Accumulated savings vs rPLA produced.

3.5. Limitations

Although functional, several design limitations were identified. The auger screw, adapted from a wood drill, lacked proper mixing sections and contributed to incomplete melt homogenisation. This led to occasional filament inconsistencies, highlighting the potential benefit of custom-machined polymer screws. Diameter control was manual, relying on operator adjustments, whereas closed-loop optical sensing could provide real-time corrections to reach commercial-grade tolerances (±0.05 mm).

Nevertheless, the modular architecture of the machine allows straightforward upgrades. Improved auger geometry, active feedback diameter sensing, and alternative drying strategies are all compatible with the current frame. Future work should also assess the impact of multiple recycling cycles, as repeated extrusion may further reduce PLA molecular weight through chain scission.

Overall, the results confirm that the proposed PLA recycling machine can reliably produce usable rPLA filament while offering significant cost savings and waste reduction, aligning with distributed recycling and additive manufacturing principles.

4. Conclusion

This study developed and evaluated a modular open-source recycling machine for producing PLA filament from waste material. The prototype integrated aluminium extrusion framing, 3D printed parts, and Arduino-based PID control to deliver continuous extrusion of recycled PLA. Energy profiling revealed that feedstock drying dominated consumption, accounting for nearly 95% of the total energy required per kilogram of filament. Nevertheless, the overall production cost of rPLA was only RM 5.31/kg, substantially lower than the RM 45/kg market price of vPLA, enabling breakeven after roughly 19 kg of filament output. These findings demonstrate that the system can reliably produce usable rPLA filament while offering significant cost savings and waste reduction. By providing an affordable and adaptable platform, the machine supports distributed recycling and sustainable additive manufacturing, contributing to broader circular economy initiatives.

Nomenclatures

A	Cross-sectional area of filament, mm^2
E_{drying}	Energy consumption for drying stage, kWh
$E_{extrusion}$	Energy consumption for extrusion stage, kWh
E_{total}	Total energy consumption per kilogram of filament, kWh

Abbreviations

FDM	Fused Deposition Modelling
PLA	Poly-lactic Acid
PID	Proportional–Integral–Derivative (control loop)
rPLA	Recycled Poly-lactic Acid
vPLA	Virgin Poly-lactic Acid

References

1. Drumright, R.E.; Gruber, P.R.; and Henton, D.E. (2000). Polylactic acid technology. *Advanced Materials*, 12(23), 1841-1846.
2. Mat Sahat, I.; Mat Rejab, M.R.; and Ma, Q. (2023). A study on 3D printing usage among Malaysian users. *Journal of Mechanical Engineering and Sciences*, 17(2), 9483-9491.
3. Auras, R.; Harte, B.; and Selke, S. (2004). An overview of polylactides as packaging materials. *Macromolecular Bioscience*, 4(9), 835-864.
4. Woern, A.L.; Byard, D.J.; Oakley, R.B.; Fiedler, M.J.; Snabes, S.L.; and Pearce, J.M. (2018). Fused particle fabrication 3-D printing: Recycled materials' optimization and mechanical properties. *Materials*, 11(8), 1413.
5. Woern, A.L.; McCaslin, J.R.; Pringle, A.M.; and Pearce, J.M. (2018). RepRapable Recyclebot: Open source 3-D printable extruder for converting plastic to 3-D printing filament. *HardwareX*, 4, e00026.
6. de Oliveira Filho, M.; de Jesus, M.C.; Nakazato, A.Z.; Kondo, M.Y.; and de Oliveira Hein, L.R. (2022). Instrumented open-source filament extruder for research and education. *HardwareX*, 12, e00362.
7. Al Rashid, A.; and Koç, M. (2023). Additive manufacturing for sustainability and circular economy: Needs, challenges, and opportunities for 3D printing of recycled polymeric waste. *Materials Today Sustainability*, 24, 100529.
8. Baechler, C.; DeVuono, M.; and Pearce, J.M. (2013). Distributed recycling of waste polymer into RepRap feedstock. *Rapid Prototyping Journal*, 19(2), 118-125.

9. Lim, L.-T.; Auras, R.; and Rubino, M. (2008). Processing technologies for poly(lactic acid). *Progress in Polymer Science*, 33(8), 820-852.
10. Mitchell, M.K.; and Hirt, D.E. (2015). Degradation of PLA fibers at elevated temperature and humidity. *Polymer Engineering & Science*, 55(7), 1652-1660.
11. Schuller, T.; Jalaal, M.; Fanzio, P.; and Galindo-Rosales, F.J. (2024). Optimal shape design of printing nozzles for extrusion-based additive manufacturing. *Additive Manufacturing*, 84, 104130.
12. Farah, S.; Anderson, D.G.; and Langer, R. (2016). Physical and mechanical properties of PLA, and their functions in widespread applications-A comprehensive review. *Advanced Drug Delivery Reviews*, 107, 367-392.
13. Murariu, M.; and Dubois, P. (2016). PLA composites: From production to properties. *Advanced Drug Delivery Reviews*, 107, 17-46.
14. Klimczuk, B.; Rudnicka, A.; Owczarek, O.; Puszkarz, A.K.; Szparaga, G.; and Puchalski, M. (2024). Investigation of the hydrolytic degradation kinetics of 3D-printed PLA structures under a thermally accelerated regime. *Materials*, 17(5), 1043.
15. Lee, S.; and Wee, J.-W. (2024). Effect of temperature and relative humidity on hydrolytic degradation of additively manufactured PLA: Characterization and artificial neural network modeling. *Polymer Degradation and Stability*, 230, 111055.
16. Quader, R.; Dramko, E.; Grewell, D.; Randall, J.; and Narayanan, L.K. (2024). Characterizing the effect of filament moisture on tensile properties and morphology of fused deposition modeled polylactic acid/polybutylene succinate parts. *3D Printing and Additive Manufacturing,* 11(3), e1151-e1161.
17. Algarni, M. (2021). The Influence of raster angle and moisture content on the mechanical properties of PLA parts produced by fused deposition modeling. *Polymers,* 13(2), 237.
18. Petsiuk, A.; and Pearce, J.M. (2021). Open source filament diameter sensor for recycling, winding and additive manufacturing machines. *Journal of Manufacturing Science and Engineering*, 143(10), 1-25.
19. Enemuoh, E.U.; Menta, V.G.; Abutunis, A.; O'Brien, S.; Kaya, L.I.; and Rapinac, J. (2021). Energy and eco-impact evaluation of fused deposition modeling and injection molding of polylactic acid. *Sustainability*, 13(4), 1875.